How to Cite: Soualmi, S., Henni, M., Djahnit, L., & Hamdani, H. (2024). Sol-gel Synthesized ZnO-$SrMn_2O_4$ Nanocomposite and Its Antibacterial Properties. *Eurasian Journal of Chemistry, 29, 4(116), 71–81*. https://doi.org/10.31489/2959-0663/4-24-12

Article

Received: 24 September 2024 | Revised: 13 November 2024 |
Accepted: 19 November 2024 | Published online: 18 December 2024

UDC 546.05

https://doi.org/10.31489/2959-0663/4-24-12

Saida Soualmi[1*], Meriem Henni[1], Leila Djahnit[2,3], Hanane Hamdani[1]

[1]*Laboratory of Synthesis and Catalysis, University of Ibn Khaldoun Tiaret, Tiaret, Algeria;*
[2]*Chemistry Department, Faculty of Exact Sciences and Informatics, University Hassiba Benbouali Chlef (UHBC), Chlef, Algeria;*
[3]*Renewable Energy and Materials Laboratory, University of Medea, Medea, Algeria*
*(*Corresponding author's e-mail: saida.soualmi@univ-tiaret.dz)*

Sol-gel Synthesized ZnO–$SrMn_2O_4$ Nanocomposite and Its Antibacterial Properties

This paper presents the synthesis of new binary oxide nanoparticles (NPs), ZnO–$SrMn_2O_4$, with a spinel structure. The sol-gel technique was used to synthesize ZnO–$SrMn_2O_4$ spinel-type oxides, which were subsequently investigated for their antibacterial properties. The NPs were characterized by a range of methods, namely Fourier transform infrared spectroscopy (FTIR), X-ray diffraction (XRD), scanning electron microscopy (SEM), and energy dispersive X-ray analysis (EDX). The FTIR analysis revealed the presence of peaks characteristic of $SrMn_2O_4$ and ZnO/$SrMn_2O_4$. These peaks confirm the presence of metal-oxygen bonds, namely Zn–O, Mn–O, and Sr–O. SEM was used to analyze the morphology, chemical composition, and size of the nanocrystals. The morphology of the particles is observed to be more irregular in shape, with a wide range of nanoparticle sizes, from 54 to 250 nm. The synthesized nanoparticles, ZnO–$SrMn_2O_4$, were used to assess their antibacterial properties against *Bacillus cereus*, *Bacillus subtilis*, *Staphylococcus aureus*, as well as *Escherichia coli* and demonstrated pronounced antibacterial efficacy. The highest antibacterial activity was recorded against *Escherichia Coli*, with a diameter range of 16–23 mm, followed by the strain *Staphylococcus aureus* with a diameter range of 13.5–27.5 mm. The next most active strain was *Bacillus subtilis*, with a diameter range of 12.5–22 mm, and *Bacillus cerus*, with a diameter range of 13.5–19 mm. Further use of the obtained ZnO–$SrMn_2O_4$ powder is recommended for application in photocatalysis of dye degradation.

Keywords: Nanocomposite, antibacterial activity, spinel, zinc oxide, Sol-gel, SEM, XRD, binary oxide.

Introduction

This paper presents the synthesis of binary oxide nanoparticles ZnO (30 %) $SrMn_2O_4$ with a spinel structure. In recent years, there has been a considerable increase in interest in nanocomposites, driven by their prospective applications in a range of fields, including public health and environmental remediation. In particular, the combination of photocatalytic and antibacterial properties offers a powerful strategy for eliminating contaminants and infections from water, air, and a range of other environments. These nanocomposites have shown promising antibacterial efficacy against both Gram-positive and Gram-negative bacterial strains, as well as strains with multidrug resistance. Thus, ZnO-based nanomaterials have been reported to be synthesized with improved antibacterial properties, especially when Au NPs are incorporated [1–5]. Moreover, researchers attributed the various trends observed for the interactions between the diverse components of the nanocomposite and the bacterial cells to the enhanced antimicrobial performance of ZnO NPs in the presence of GO or RGO [6]. The synthesis and design of MnO and ZnO nanoparticles have resulted in the preparation of new MnO/ZnO nanocomposites with marked antibacterial efficacy. These nanocomposites have demonstrated high inhibition rates against *E. coli* and other pathogenic bacteria, indicating that they play a vital role in overcoming bacterial resistance [7]. Further research is required to synthesize the $ZnMn_2O_4$/ZnO nanocomposite for antibacterial purposes, as the existing research base for new materials claiming improved antimicrobial efficiency is insufficient. Previous research indicates that the synthesis of nanocomposites comprising zinc oxide nanoparticles and manganese (II) oxide enhances the antibacterial properties of the nanoparticles [8]. Moreover, numerous other nanocomposites, including Fe_3O_4/ZnO-based materials, have demonstrated noteworthy antibacterial properties, suggesting potential applications in the management of bacterial infections [9]. Previous research established candidature-level reactions in ZnO and $MnWO_4$, and both of these nanoparticles show potent antibacterial results. The synthesis of ZnO nanoparticles has been optimized for antibacterial properties, considering synthesis parameters [10]. The nanostructures of ZnO surfaces possess great antibacterial activity, which causes bacterial cell lysis in microfluidic devices [11]. In contrast, MnO_2 nanoparticles have been demonstrated to exhibit antibacterial and anti-

biofilm properties against quinolone-resistant gram-positive and negative pathogenic bacteria, including *S. aureus* and *E. coli* [12]. It is conceivable that a synergistic effect may be observed between ZnO and $MnWO_4$, which could result in an enhanced antibacterial activity of the composite material. Further research into the antibacterial efficacy of a composite material comprising ZnO doped with $SrMn_2O_4$ could facilitate the modification and enhancement of the efficiency of the antibacterial agents employed in the medical field, as well as other professional contexts. ZnO nanoparticles have demonstrated high antibacterial efficacy due to a number of mechanisms, including the liberation of Zn^{+2}, the generation of reactive oxygen species (ROS), and the intercalation of microbial cell membranes [13]. Furthermore, the antibacterial efficacy of ZnO nanomaterials can be enhanced through the formation of composites with other materials, such as $SrMn_2O_4$, which has the potential to markedly inhibit the recombination of electrons and holes [14]. The literature indicates that ZnO and Mn-doped ZnO nanoparticles, when immobilized on titanium implants, are effective against the majority of bacterial profiles. Furthermore, the $Zn_xMn_{(1-x)}O$@Ti hybrids have been shown to outperform ZnO@Ti [15]. The results of this research study allow us to hypothesise that the addition of ZnO with other materials, such as $SrMn_2O_4$, and the introduction of metal ions, including Mn, will enhance the creation of more effective antibiotics with the potential to combat microbial antibiotic resistance.

Experimental

Materials used

Strontium nitrate ($Sr(NO_3)_2$), manganese (II) nitrate hydrate ($Mn(NO_3)_2{\cdot}4H_2O$), zinc acetate ($Zn(O_2CCH_3)_2{\cdot}2H_2O$), sodium hydroxide (NaOH), ethanol and Acid citric were purchased from Sigma Aldrich. Fourier transform infrared (FT-IR) spectra were recorded using an FTIR-8400 type SHIMADZU spectrometer. The measurement of X-ray diffraction patterns was carried out using a Rigaku MINIFLEX 600 diffractometer. The products morphology was determined using scanning electron microscopy (SEM) techniques on the SEM-QUANTA 650 FEI.

Synthesis of ZnO nanoparticles

In order to synthesize ZnO nanoparticles, a solution of $Zn(NO_3)_2{\cdot}6H_2O$ (250 mL, 0.2 M) and a solution of NaOH (250 mL, 0.5 M) were prepared with deionized water. The sodium hydroxide solution was added dropwise using a burette to the zinc acetate solution at room temperature. This was achieved by stirring vigorously until a pH of 12 was reached. This resulted in the formation of a white precipitate of zinc hydroxide ($Zn(OH)_2$), which was separated by centrifugation for 30 min and washed three times with distilled water and then ethanol. The resulting product was dried at 60 °C in an air atmosphere for 24 hours to convert $Zn(OH)_2$ into ZnO NPs.

Synthesis of $SrMn_2O_4$ nanoparticles

The synthesis of $SrMn_2O_4$ NPs involved the dissolution of 1.571 g of ($Sr(NO_3)_2$) in 40 ml of ethanol. Conversely, 4.713 g of manganese nitrate (II) hydrate ($Mn(NO_3)_2{\cdot}4H_2O$) was dissolved in 110 ml of ethanol. The two solutions previously obtained were added, in a dropwise manner, to a solution of citric acid, which was prepared by dissolving 5.106 g of $C_6H_8O_7$ in 100 ml of demineralized water. Subsequently, the solution was heated to 80 °C for a period of three hours, with stirring using a magnetic stirrer.

The solution underwent evaporation, forming a gel that was subsequently subjected to drying at 60 °C and calcination at 700 °C for four hours. This process resulted in the formation of $SrMn_2O_4$ nanocomposites, as illustrated in Figure 1.

Figure 1. Preparation of ZnO (30 %) $SrMn_2O_4$ using the sol gel method.

Synthesis of ZnO (30 %) $SrMn_2O_4$ nanocomposites

In order to develop ZnO (30 %) $SrMn_2O_4$ nanocomposite powders, the same synthesis protocol for $SrMn_2O_4$ must be followed, with the exception that the previous solutions are mixed with the incorporation of ZnO 30 % (molar percentage).

Results and Discussion

To explain the phase structure and the degree of crystallinity of the synthesized products X-ray diffraction was used. The XRD pattern of the prepared samples is presented in Figure 2. The reflection peaks observed at values of 25°, 60.63°, 33.39°, 36.73°, 45.06°, 50.48°, 59.61°, and 61.45° correspond to the data of JCPDS n°96-400-1312 and card n° JCPDS 96-9007521. The prepared sample of ZnO NPs corresponds to the JCPDS card n°96.101-1259. XRD data confirm formation of ZnO.

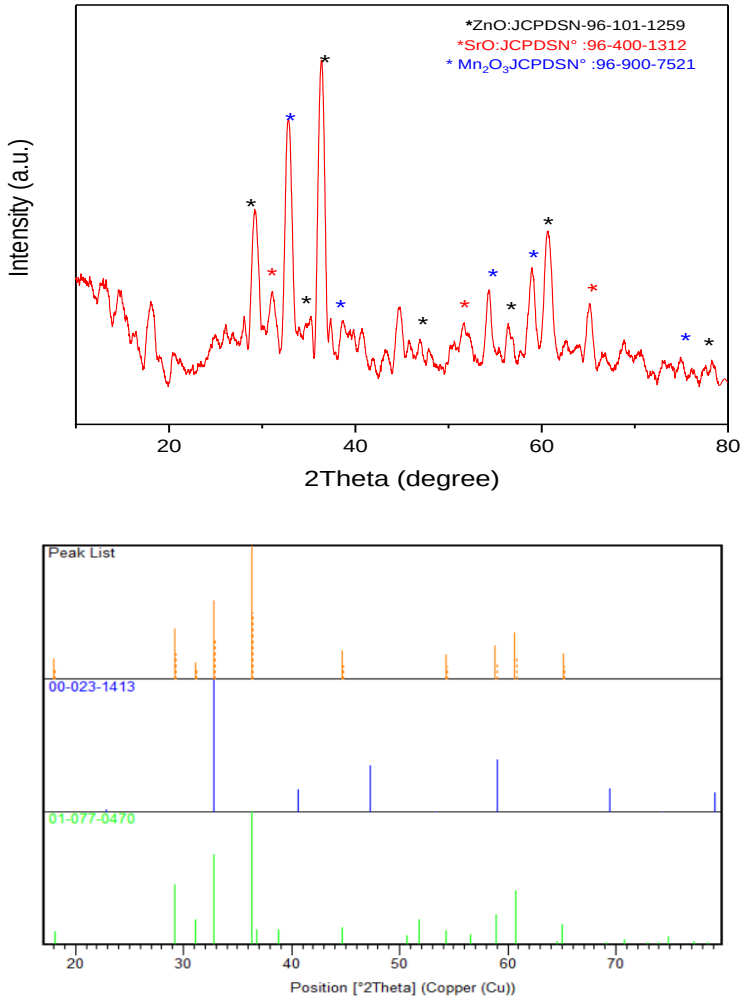

Figure 2. XRD pattern of $SrMn_2O_4$ with Reference number

In the case of ZnO (30 %) $SrMn_2O_4$, the reflected peaks were observed at 25°, 60.63°, 33.39°, 36.73°, 45. 06°, 50. 48°, 59. 61°, and 61. 45°, corresponding to plans (101), (112), (103), (202), (220), (204), (321), and (224) (Fig. 3).

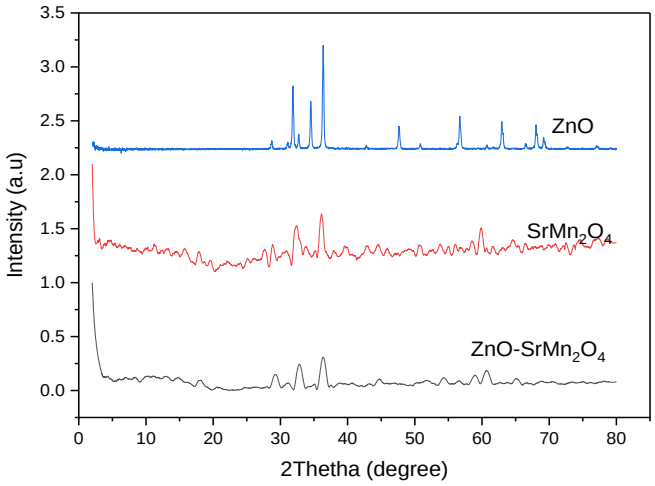

Figure 3. XRD pattern of ZnO, $SrMn_2O_4$ and ZnO (30 %) $SrMn_2O_4$

The Scherrer equation [16], which is Dc = Kλ/β cosθ, was used for the calculation of crystallites. In this formula, β represents the width of the observed diffraction peak at half of its maximum height, also known as FWHM, which stands for full width at half maximum. K is the shape factor, its value varies and it is approximately equal to 0.9 and λ is the X-ray wavelength (CuK_α radiation, which is equal to 0.154 nm). From the Scherrer equation, the average crystalline sizes were found to be 42 nm for ZnO, 13 nm for $SrMn_2O_4$, and 20 nm for the ZnO (30 %) $SrMn_2O_4$ composite, respectively.

The FTIR spectra for ZnO, $SrMn_2O_4$, and ZnO (30 %) $SrMn_2O_4$ are presented in (Fig. 4) below. In the case of ZnO, the stretching vibration of the Zn–O bond is related to the peak at 498.75 cm^{-1}. In the case of $SrMn_2O_4$, the large peak observed at approximately 512.85 cm^{-1} is due to the vibration of the Mn-O functional group, which is associated with the tetrahedral coordination of MnO_2 ions. Bands at approximately 611.52 cm^{-1} correspond to stretching vibrations of Sr–O [17]. The presence of peaks for $SrMn_2O_4$ and ZnO/$SrMn_2O_4$ confirm the existence of metal-oxygen bonds (Zn–O, Mn–O, and Sr–O). A less intense band appears approximately at 3500 cm^{-1}, which can be attributed to the stretching vibration of the O–H group originating from H_2O molecules adsorbed on the surface of the material. Another peak was identified at 1600 cm^{-1}, which is attributed to O–H bending vibrations.

In the case of ZnO (30 %) $SrMn_2O_4$ (Fig. 4), a shift in the FTIR peaks was observed, which is frequently associated with alterations in the bond lengths and bond angles within the crystal structure. ZnO can cause a change in the vibrational frequencies of Sr-O bonds, a phenomenon that is frequently observed by FTIR. This shift is a consequence of the substitution of Zn^{2+} ions within the structure, which results in alterations to the intermediate distances and bond strengths.

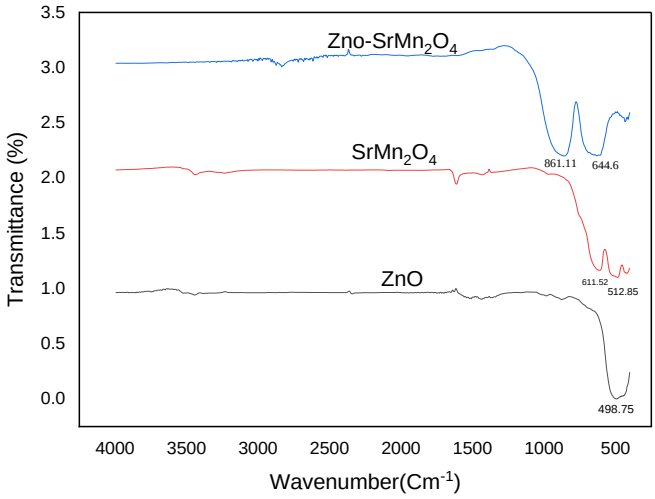

Figure 4. FTIR spectra of ZnO nanoparticles, $SrMn_2O_4$ and ZnO (30 %) $SrMn_2O_4$.

Figure 5 illustrates the morphology of the particles, which exhibit a more irregular shape and a wide range of nanoparticle sizes, spanning from 54 to 250 nm.

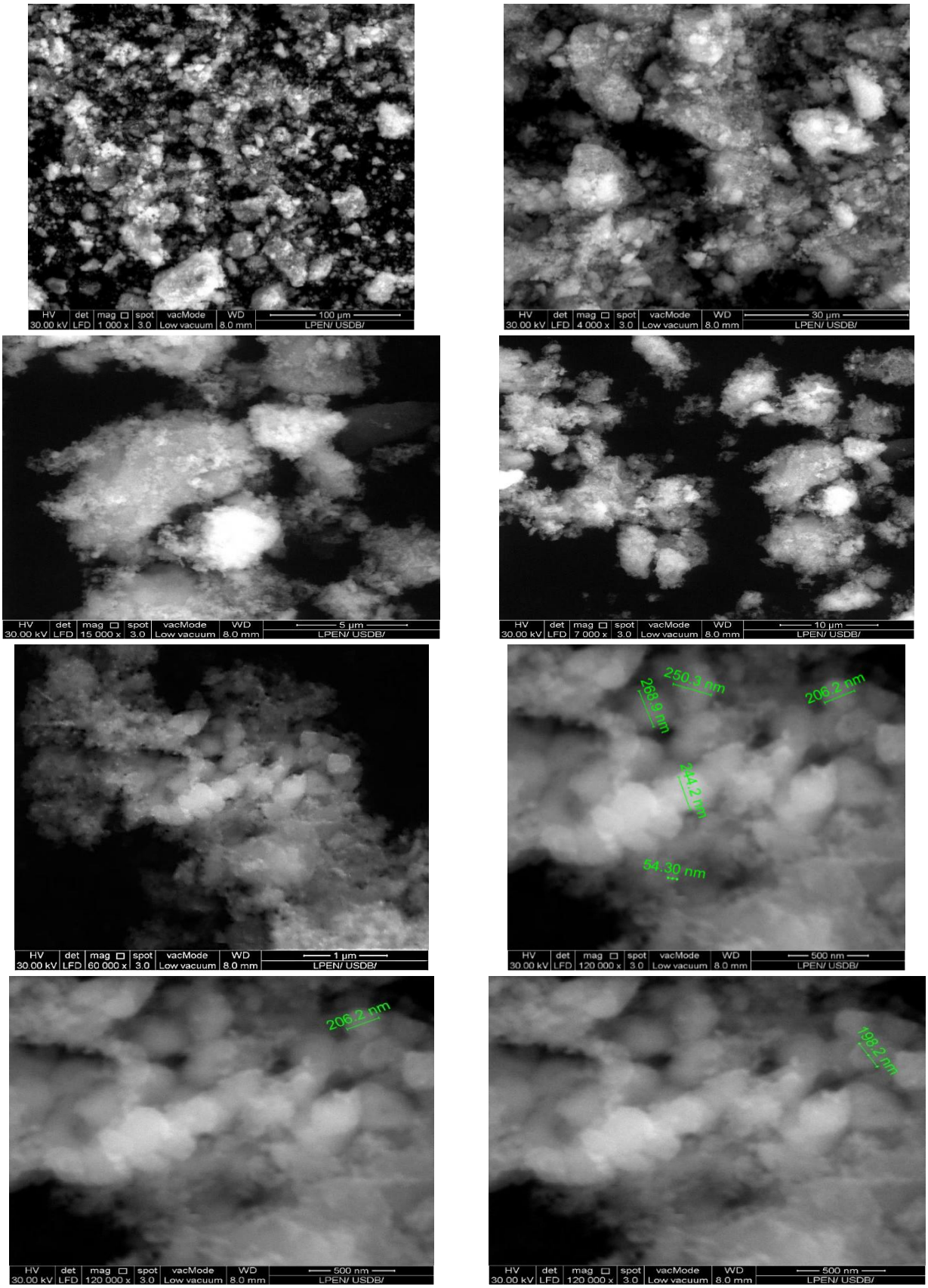

Figure 5. SEM micrograph of ZnO (30 %) $SrMn_2O_4$ NPs

Energy dispersive X-ray (EDX) analysis was used to examine the chemical components of the produced nanoparticles, which revealed the presence of zinc, oxygen, Sr and Mn atoms (Fig. 6). Table 1 presents the atomic percentages of each element. These results demonstrate that the ZnO sample (30 %) $SrMn_2O_4$ contains amounts of Sr, Zn, Mn, and O. Additionally, carbon was detected, originating from the support where the material used during the EDX manipulation was deposited.

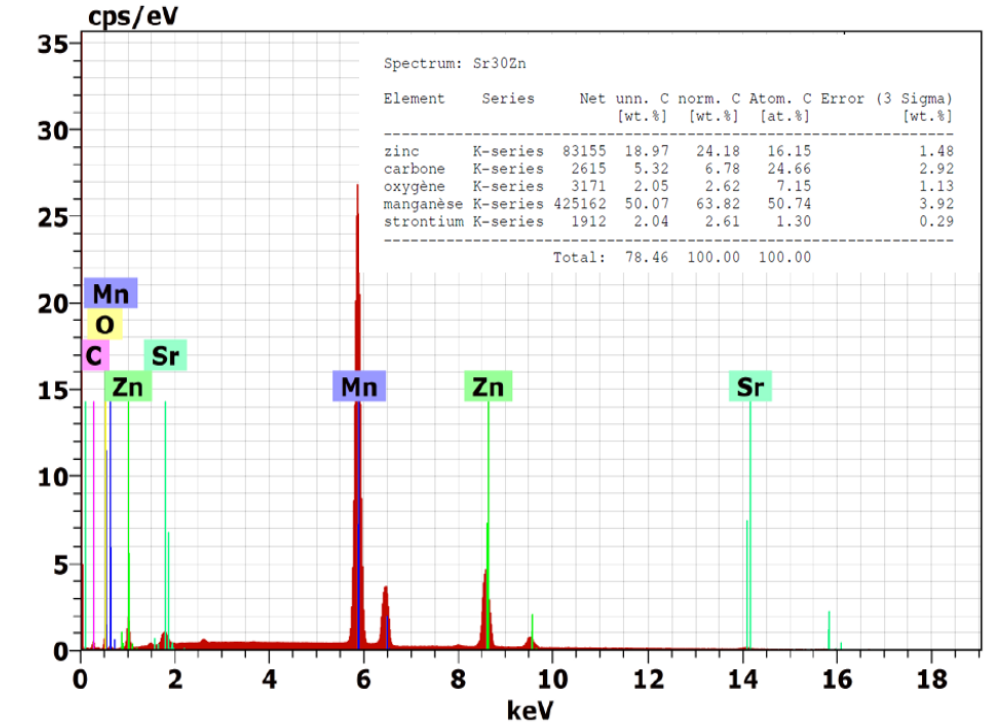

Figure 6. EDX images of synthesized ZnO (30 %) $SrMn_2O_4$ NPs

Antibacterial activity

The antibacterial activity of ZnO (30 %) $SrMn_2O_4$ nanoparticles was determined using the well diffusion method [18, 19]. An 18-hour culture of Gram-positive (*Bacillus cereus* (ATCC10876), *Bacillus subtilis* (ATCC 6633), and *Staphylococcus aureus* (ATCC 25925)) and Gram-negative (*Escherichia coli* (ATCC 25922)) strains was adjusted to 0.5 McFarland. Freshly prepared Mueller-Hinton agar plates were inoculated with 100 µl of bacterial suspension. Four wells of 8 mm in diameter were created on the agar plates. Subsequently, 100 µl of ZnO (30 %) $SrMn_2O_4$ nanoparticles of different concentration were added to each well. Then, the Petri dishes were left at 4 °C for 30 min for good diffusion of the nanoparticles. The plates were incubated at 37 °C for 24 hours. Inhibition zones were measured in millimetres.

The antibacterial activity of the ZnO (30 %) $SrMn_2O_4$ nanoparticles was confirmed by the appearance of clear zones around the wells (Fig. 7).

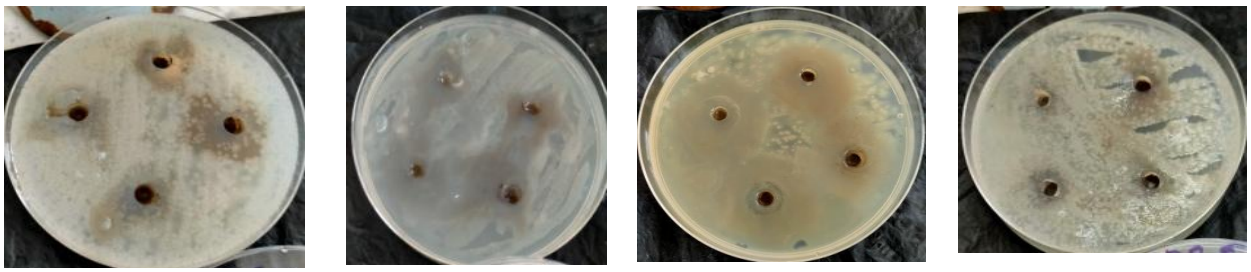

B. cereus *E. coli* *S. aureus* *B. subtilis*

Figure 7. Results of the antibacterial activity of ZnO (30 %) $SrMn_2O_4$

The diameters of the inhibition zones of the nanoparticles against Gram-positive and Gram-negative bacteria are presented in Figure 8 and Table 1. These results demonstrate the effective inhibitory effect of the synthesized nanoparticles. Furthermore, the highest antibacterial activity was observed against *Escherichia Coli*, with a diameter ranging between 16 and 23 mm, followed by the strain *Staphylococcus aureus*, with a diameter ranging from 13.5 to 27.5 mm, *Bacillus subtilis* with a diameter ranging from 12.5 to 22 mm and *Bacillus cereus* with a diameter ranging from 13.5 to 19 mm. These data affirm that the increase in the concentration of $SrMn_2O_4$ 30 %ZnO nanoparticles is accompanied by the increase in inhibition of the growth of these bacteria. Furthermore, this variation in activity can be attributed to the structural variations in the cell walls of the pathogenic strains selected and also to the size, morphology and composition of the nanoparticles under consideration.

Additionally, the mechanism of antimicrobial action of nanoparticles is generally described as adhering to one of three models: induction of oxidative stress [20], the release of metal ions [21] or non-oxidative mechanisms [22]. It is possible for all three types of mechanisms to occur simultaneously.

The findings of our research indicate that $SrMn_2O_4$ 30 %ZnO nanoparticles exhibit considerable efficacy in combating pathogens. The nanoparticles function in a manner analogous to other compounds, including ZnO/$SrZnO_2$ and $ZnMn_2O_4$-chitosan. The synthesis of these nanoparticles was carried oud using sol-gel methods. [23–26]. These compounds have been demonstrated to be highly effective in the killing of bacteria, including *E. coli*, *S. aureus*, and *P. aeruginosa*. The *E. coli* demonstrated greater susceptibility to the ZnO/$SrZnO_2$ composite than either oxide individually, as it relies on pure ZnO or $SrZnO_2$ oxide for normal cellular activity.

ZnO–SnO_2 nanoparticles demonstrated pronounced antibacterial activity against Staphylococcus aureus, Streptococcus mutans, and Escherichia coli. The efficacy of the nanoparticles was demonstrated at both high and low concentrations. The ZnO–CuO composite particles were also observed to exhibit antibacterial activity against both gram-positive and gram-negative bacteria. The nanoparticles were tested against a range of bacteria, including Staphylococcus aureus, E. coli, and Pseudomonas aeruginosa.

Table 1

Zone of inhibition of $SrMn_2O_4$-ZnO against bacterial strains

Microorganisms	ZnO (30 %) $SrMn_2O_4$ NPs			
	2(mg/ml)	5(mg/ml)	8(mg/ml)	10(mg/ml)
Staphylococcus aureus	13.5	14	15	27.5
Bacillus subtilis	12.5	14	15	22
Escherichia coli	16	18	22	23
Bacillus cerus	13.5	16	18	19

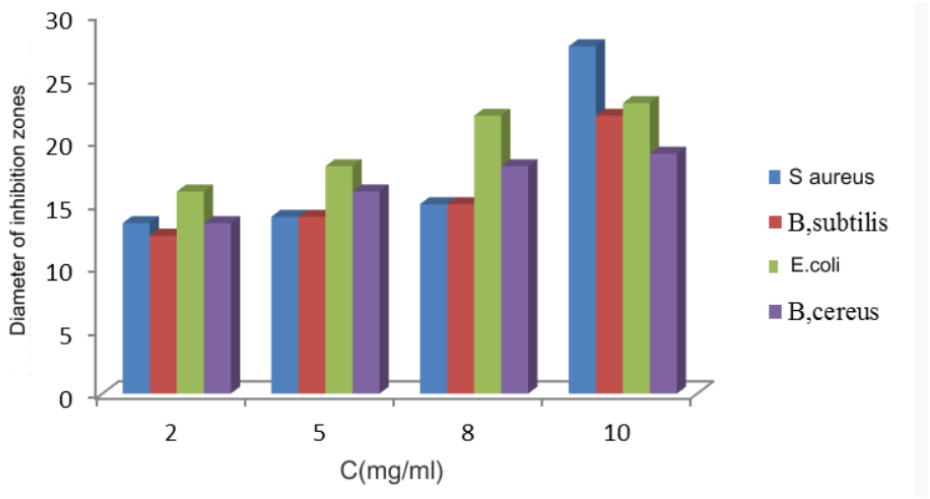

Figure 8. Antimicrobial activity of ZnO (30 %) $SrMn_2O_4$ nanoparticles

Table 2

Comparison of results with published data nanoparticles

Nanocomposite	Antimicrobial Activity	Effective Bacteria/Fungi	Mechanism	Average particle sizes	Stability	Ref.
ZnO	99.99 % 99.63 %	*E. coli* *S. aureus* *B. cinerea*	ROS, Disruption of Cell Membrane Integrity	20–40 nm	Size and Surface Area Effects and Role of Plant Extracts	27
ZnO	significant	*E.coli* and *S. aureus* *A. nige*	Physical and chemical interactions like Electrostatic Effects: Membrane Abrasion and ROS	nanoporous	Surface Area Effects	28
ZnO–Ag	higher	against *E. coli* compared to *S. aureus*	Membrane Disruption and ROS, Inhibition of Cellular Functions and Multitarget Mechanism	14.8 nm	pH range of 7-8 increasing Ag concentrations ameliore stability in various environments	29
Zn–CuO	superior	*S. aureus* and *E. coli*	ROS and Cell Membrane Disruption	8 nm to 25.58 nm	Stabilization by Vaccinium arctostaphylos L. fruit extract Zingiber officinale Rhizome Extract	30, 31
ZnO/TiO_2	significant	*Staphylococcus aureus* and Gram-negative bacteria (*Escherichia coli, Pseudomonas aeruginosa, Klebsiella pneumoniae, Salmonella Paratyphi A*) as well as fungi (*Candida albicans, Aspergillus flavus*)	The antimicrobial mechanism is primarily attributed to the production of reactive oxygen species (ROS), which induce oxidative stress and apoptosis in microbial cells	30 to 100 nm	/	32
MnO/ZnO	High Inhibition Rate: The MnO/ZnO-2.5 % nanocomposite 92.3 %	Achieving an inhibition rate against *E. coli*	ROS Damage to Bacterial Cells Photocatalytic Activity	/	Synergistic Effects of Doping:	33
Our research	Significant	*S. aureus* *B. subtilis* *E. coli* B. cerus	ROS, release of metal ions, non-oxidative mechanisms	Particles in a more irregular shape with a wide (54-250)	Stabilization by citric acid	

Conclusions

In conclusion, the sol-gel process for the synthesis of ZnO, $SrMn_2O_4$, and ZnO (30 %) $SrMn_2O_4$ nanostructures has been described in detail above. The characterization of the developed samples was carried out using FTIR, SEM, EDX, and XRD. The synthesised nanostructures were employed to assess their antibacterial characteristics, and the results demonstrated that the $SrMn_2O_4$30 %ZnO NPs exhibited a pronounced pathogen-suppressing capacity. It is recommended that the ZnO-$SrMn_2O_4$ powder be employed further for the photocatalytic degradation of dyes. The ZnO/$SrZnO_2$ material demonstrated a notable photocatalytic effect for the degradation of Congo red dye after 80 minutes of UV/vis irradiation [23], and as an electrode material in supercapacitors, as evidenced by the NiO/$ZnMn_2O_4$ materials, which exhibited a specific capacity [34].

*Author Information**

**The authors' names are presented in the following order: First Name, Middle Name and Last Name*

Saida Soualmi (*corresponding author*) — Doctor and Researcher, Laboratory of Synthesis and Catalysis, University of Ibn Khaldoun Tiaret, 14000, Tiaret, Algeria; *e-mail*: saida.soualmi@univ-tiaret.dz; https://orcid.org/0009-0009-4858-8695

Meriem Henni — Doctor and Researcher, Laboratory of Synthesis and Catalysis, University of Ibn Khaldoun Tiaret, 14000, Tiaret, Algeria; *e-mail*: hanan1112@yahoo.fr, https://orcid.org/0009-0005-5378-0674

Leila Djahnit — Doctor and Researcher, Chemistry Department, Faculty of Exact Sciences and Informatics, University Hassiba Benbouali Chlef (UHBC), 02000, Chlef, Algeria; Renewable Energy and Materials Laboratory, University of Medea, 26000, Medea, Algeria; *e-mail*: Leila_djahnit@yahoo.fr, https://orcid.org/0000-0001-5834-8024

Hanane Hamdani — Master Student. Chemistry Department, Laboratory of Synthesis and Catalysis, University of Ibn Khaldoun Tiaret, 14000, Algeria; *e-mail*: hananehamdani25@gmail.com

Author Contributions

The manuscript was written through contributions of all authors. All authors have given approval to the final version of the manuscript: **Saida Soualmi** conceptualization, data curation, investigation, methodology, validation, visualization, writing-review & editing; **Meriem Henni** application of the antibacterial activity of the synthesized materials; **Leila Djahnit** conservation of antibacterial activity data, **Hanane Hamdani** synthesis of material.

Conflicts of Interest

The authors declare no conflict of interest.

References

1 Behera, S. K., Huwaikem, M., Jena, B., Shah, M. P., Chakrabortty, S., Tripathy, S. K., & Mishra, A. (2023). Fabrication of ZnO/Gypsum/Gelatine nanocomposites films and their antibacterial mechanism against Staphylococcus aureus. *Biotechnology and Genetic Engineering Reviews*, 1–24. https://doi.org/10.1080/02648725.2023.2216419

2 Krishnan, M., Subramanian, H., Ramachandran, S. K., Muthukumarasamy, A., Ramadoss, D., Mahalingam, A., ... & Hwang, J. S. (2023). Synthesis of bimetallic $BiPO_4$/ZnO nanocomposite: enhanced photocatalytic dye degradation and antibacterial applications. *International Journal of Molecular Sciences*, *24*(3), 1947. https://doi.org/10.3390/ijms24031947

3 Dediu, V., Busila, M., Tucureanu, V., Bucur, F. I., Iliescu, F. S., Brincoveanu, O., & Iliescu, C. (2022). Synthesis of ZnO/Au Nanocomposite for Antibacterial Applications. *Nanomaterials, 12*(21), 3832. https://doi.org/10.3390/nano12213832

4 Sreekanth, R., Kumar, S. N., Reddy, M., Pattar, J., & BV, D. R. (2024). Investigating the effect of acidic and basic precipitation on the antibacterial activity of ZnO nanoparticles against Gram-negative and Gram-positive bacteria. *Journal of Materials Chemistry B, 12*(8), 2180–2196. https://doi.org/10.1039/d3tb02119j

5 Alshammari, E. M., Sherwani, S., Alqahtani, F. O., Khan, M., Khan, W. A., Khan, M. W. A., Alsukaibi, A. K. D., Al-Motair, K., Alenezi, K. M., & Umar, A. (2023). Green Synthesis of Novel Antimicrobial ZnO Nanorods. *Science of Advanced Materials, 15*(8), 1000–1005. https://doi.org/10.1166/sam.2023.4517

6 Ahmadi, R., Fattahi Nafchi, R., Sangpour, P., Bagheri, M., & Badiei, E. (2023). A comparative study: Green synthesis and evaluation of ZnO-GO and ZnO-RGO nanocomposites for antibacterial applications. *Materials Science and Engineering: B*, 294, 116555. https://doi.org/10.1016/j.mseb.2023.116555

7 Kong, J., Zhang, J., Shen, M., Zhang, S., Shen, P., & Ren, C. (2022). Preparation of manganese(II) oxide doped zinc oxide nanocomposites with improved antibacterial activity via ROS. Chemical Physics Letters, 806, 140053. https://doi.org/10.1016/j.cplett.2022.140053

8 Hussain Shah, M. B., Mansoor, Q., Jan, T., Farooq, Z., & Ilyas, S. Z. (2023). Synthesis of SnO_2 nanoparticles coated ZnO–g–C_3N_4 composite nanostructures with novel antibacterial activity. *Zeitschrift Für Naturforschung A, 78*(6), 557–562. https://doi.org/10.1515/zna-2023-0032

9 Alasmari, A., Alshehri, K., Azab, A. A., & Solyman, S. (2024). Detailed investigation of the structural and electrical properties of ZnO/Fe_3O_4 nanocomposites. *Physica Scripta, 99*(3), 035921. https://doi.org/10.1088/1402-4896/ad21c9

10 Narang, K., Kumar, J., Saxena, S., Chaudhary, M., Narender, & Chandwani, G. (2024). Smart Computing Optimization of the Bactericidal Potential of ZnO Nanoparticles: A Support Vector Machine Approach. *2024 IEEE International Conference on Computing, Power and Communication Technologies (IC2PCT)*, 1635–1639. https://doi.org/10.1109/ic2pct60090.2024.10486492

11 Xesfyngi, Y., Georgoutsou-Spyridonos, M., Tripathy, A., Milionis, A., Poulikakos, D., Mastellos, D. C., & Tserepi, A. (2023). A High-Performance Antibacterial Nanostructured ZnO Microfluidic Device for Controlled Bacterial Lysis and DNA Release. *Antibiotics*, *12*(8), 1276. https://doi.org/10.3390/antibiotics12081276

12 AboKsour, M. F., Al-Marjani, M. F., & Rheima, A. M. (2024). Preparation and Effects of Manganese Oxide Nanoparticles Against Quinolone-Resistant Bacteria Isolated from Hospital Wastewater. *Al-Rafidain Journal of Medical Sciences* (ISSN 2789-3219), *6*(2), 94–100. https://doi.org/10.54133/ajms.v6i2.728

13 Gudkov, S. V., Burmistrov, D. E., Serov, D. A., Rebezov, M. B., Semenova, A. A., & Lisitsyn, A. B. (2021). A Mini Review of Antibacterial Properties of ZnO Nanoparticles. *Frontiers in Physics*, 9. https://doi.org/10.3389/fphy.2021.641481

14 Abebe, B., Zereffa, E. A., Tadesse, A., & Murthy, H. C. A. (2020). A Review on Enhancing the Antibacterial Activity of ZnO: Mechanisms and Microscopic Investigation. *Nanoscale Research Letters*, *15*(1). https://doi.org/10.1186/s11671-020-03418-6

15 Calabrese, G., De Luca, G., Franco, D., Morganti, D., Rizzo, M. G., Bonavita, A., ... & Conoci, S. (2023). Structural and antibacterial studies of novel ZnO and $Zn_xMn_{(1-x)}O$ nanostructured titanium scaffolds for biomedical applications. *Biomaterials Advances*, *145*, 213193. https://doi.org/10.1016/j.bioadv.2022.213193

16 Syah, R., Hussein Altajer, A., F Abdul-Rasheed, O., Amri Tanjung, F., M Aljeboree, A., Abd Alrazzak, N., & F Alkaim, A. (2021). $CuMoO_4$/ZnO nanocomposites: novel synthesis, characterization, and photocatalytic performance. *Journal of Nanostructures*, *11*(1), 73–80.

17 Vázquez-Olmos, A., Redón, R., Rodríguez-Gattorno, G., Esther Mata-Zamora, M., Morales-Leal, F., Fernández-Osorio, A. L., & Saniger, J. M. (2005). One-step synthesis of Mn3O4 nanoparticles: Structural and magnetic study. *Journal of Colloid and Interface Science*, *291*(1), 175–180. https://doi.org/10.1016/j.jcis.2005.05.005

18 Vahidi, H., Kobarfard, F., Kosar, Z., Mahjoub, M. A., Saravanan, M., & Barabadi, H. (2020). Mycosynthesis and characterization of selenium nanoparticles using standard penicillium chrysogenum PTCC 5031 and their antibacterial activity: A novel approach in microbial nanotechnology. *Nanomed. J*, *7*(4), 315–323. https://doi.org/10.22038/nmj.2020.07.00008

19 Bhat, K. G., & Nalawade, T. M. (2016). Antimicrobial Activity of Endodontic Medicaments and Vehicles using Agar Well Diffusion Method on Facultative and Obligate Anaerobes. *International Journal of Clinical Pediatric Dentistry*, *9*(4), 335–341. https://doi.org/10.5005/jp-journals-10005-1388

20 Gurunathan, S., Han, J. W., Dayem, A. A., Eppakayala, V., & Kim, J. H. (2012). Oxidative stress-mediated antibacterial activity of graphene oxide and reduced graphene oxide in Pseudomonas aeruginosa. *International journal of nanomedicine*, 5901–5914. https://doi.org/10.2147/IJN.S37397

21 Nagy, A., Harrison, A., Sabbani, S., Munson Jr, R. S., Dutta, P. K., & Waldman, W. J. (2011). Silver nanoparticles embedded in zeolite membranes: release of silver ions and mechanism of antibacterial action. *International journal of nanomedicine*, 1833–1852. https://doi.org/10.2147/IJN.S24019

22 Leung, Y. H., Ng, A. M. C., Xu, X., Shen, Z., Gethings, L. A., Wong, M. T., Chan, C. M. N., Guo, M. Y., Ng, Y. H., Djurišić, A. B., Lee, P. K. H., Chan, W. K., Yu, L. H., Phillips, D. L., Ma, A. P. Y., & Leung, F. C. C. (2013). Mechanisms of Antibacterial Activity of MgO: Non-ROS Mediated Toxicity of MgO Nanoparticles Towards Escherichia coli. *Small*, *10*(6), 1171–1183. Portico. https://doi.org/10.1002/smll.201302434

23 Ahmad, M. Aadil, S.R. Ejaz, M. Akhtar, H. Noor, S. Haider, Ibrahim A. Alsafari, Ghazalah Yasmin (2022.). Sol-gel synthesis of nanostructured ZnO/$SrZnO_2$ with boosted antibacterial and photocatalytic activity. *Ceramics International*, *48*, 2, 2394–2405. https://doi.org/10.1016/j.ceramint.2021.10.020

24 Packirisamy, R. G., Govindasamy, C., Sanmugam, A., Karuppasamy, K., Kim, H.-S., & Vikraman, D. (2019). Synthesis and Antibacterial Properties of Novel $ZnMn_2O_4$–Chitosan Nanocomposites. *Nanomaterials*, *9*(11), 1589. https://doi.org/10.3390/nano9111589

25 Bandekar, S. S., Hosamane, S. N., Patil, C., Yaragatti, A., Hukerikar, A., Patil, S., & Chachadi, P. (2020). ZnO-CuO nanocomposites: synthesis, characterization and antibacterial activity. *Journal of Physics: Conference Series*, *1706*(1), 012018. https://doi.org/10.1088/1742-6596/1706/1/012018

26 Kumar, A. A., & Jain, R. K. (2024). Synthesis and Characterization of the Zinc-Oxide: Tin-Oxide Nanoparticle Composite and Assessment of Its Antibacterial Activity: An In Vitro Study. *Cureus*. https://doi.org/10.7759/cureus.53016

27 Ma, W., Zhu, G., Zhang, Y., & Guo, J. (2024). Green synthesis of ZnO NPs with long-lasting and ultra-high antimicrobial activity. *Surfaces and Interfaces*, *50*, 104506. https://doi.org/10.1016/j.surfin.2024.104506

28 de Lucas-Gil, E., Leret, P., Monte-Serrano, M., Reinosa, J. J., Enríquez, E., Del Campo, A., Cañete, M., Menéndez, J., Fernández, J. F., & Rubio-Marcos, F. (2018). ZnO Nanoporous Spheres with Broad-Spectrum Antimicrobial Activity by Physicochemical Interactions. *ACS Applied Nano Materials*, *1*(7), 3214–3225. https://doi.org/10.1021/acsanm.8b00402

29 Mtavangu, S. G., Machunda, R. L., van der Bruggen, B., & Njau, K. N. (2022). In situ facile green synthesis of Ag–ZnO nanocomposites using Tetradenia riperia leaf extract and its antimicrobial efficacy on water disinfection. *Scientific Reports*, *12*(1). https://doi.org/10.1038/s41598-022-19403-1

30 Mohammadi-Aloucheh, R., Habibi-Yangjeh, A., Bayrami, A., Latifi-Navid, S., & Asadi, A. (2018). Enhanced anti-bacterial activities of ZnO nanoparticles and ZnO/CuO nanocomposites synthesized using *Vaccinium arctostaphylo*s L. fruit extract. *Artificial Cells, Nanomedicine, and Biotechnology*, *46*(sup1), 1200–1209. https://doi.org/10.1080/21691401.2018.1448988

31 Takele, E., Feyisa Bogale, R., Shumi, G., & Kenasa, G. (2023). Green Synthesis, Characterization, and Antibacterial Activity of CuO/ZnO Nanocomposite Using Zingiber officinale Rhizome Extract. *Journal of Chemistry*, *2023*, 1–15. https://doi.org/10.1155/2023/3481389

32 Pang, S., He, Y., Zhong, R., Guo, Z., He, P., Zhou, C., Xue, B., Wen, X., & Li, H. (2019). Multifunctional ZnO/TiO_2 nanoarray composite coating with antibacterial activity, cytocompatibility and piezoelectricity. *Ceramics International*, *45*(10), 12663–12671. https://doi.org/10.1016/j.ceramint.2019.03.076

33 Kong, J., Zhang, J., Shen, M., Zhang, S., Shen, P., & Ren, C. (2022). Preparation of manganese(II) oxide doped zinc oxide nanocomposites with improved antibacterial activity via ROS. *Chemical Physics Letters*, *806*, 140053. https://doi.org/10.1016/j.cplett.2022.140053

34 Pearline, C. L., Abel, M. J., Pramothkumar, A., Senthilkumar, N., Anbalagan, P., & Prince, J. J. (2020). Investigation on structural, optical and electrochemical behavior of NiO/$ZnMn_2O_4$ ternary nanocomposites via two-step synthesis approach for supercapacitor application. *Chemical Papers*, *75*(2), 641–651. https://doi.org/10.1007/s11696-020-01258-3